NASA Technical Memorandum 4144

Performance Potential of an Advanced Technology Mach 3 Turbojet Engine Installed on a Conceptual High-Speed Civil Transport

Shelby J. Morris, Jr., Karl A. Geiselhart, and Peter G. Coen

NOVEMBER 1989

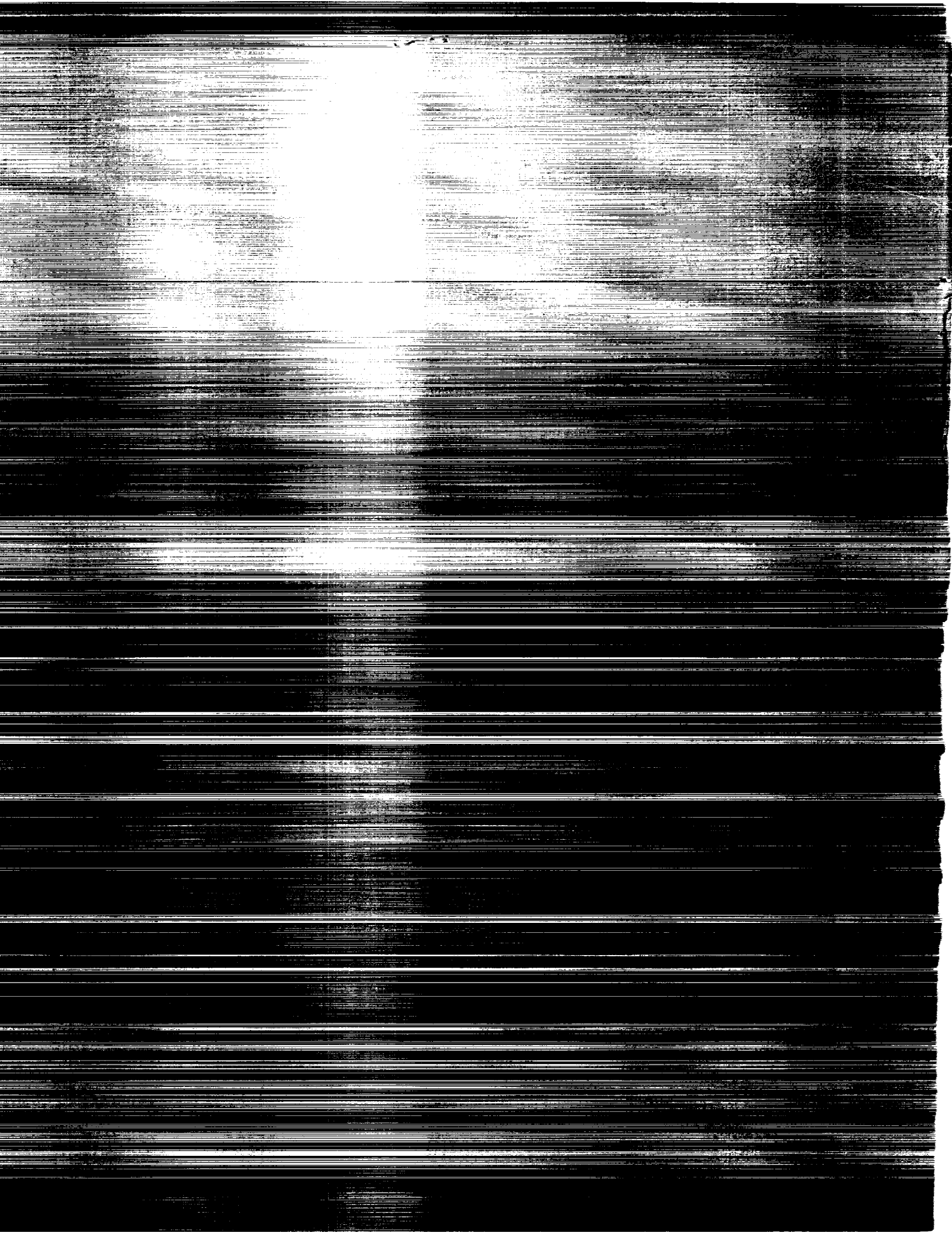

NASA Technical Memorandum 4144

Performance Potential of an Advanced Technology Mach 3 Turbojet Engine Installed on a Conceptual High-Speed Civil Transport

Shelby J. Morris, Jr.
Langley Research Center
Hampton, Virginia

Karl A. Geiselhart
PRC Kentron, Inc.
Aerospace Technologies Division
Hampton, Virginia

Peter G. Coen
Langley Research Center
Hampton, Virginia

National Aeronautics and
Space Administration
Office of Management
Scientific and Technical
Information Division

1989

Summary

The performance of an advanced technology, conceptual turbojet engine optimized for a high-speed civil aircraft is presented. This information represents an estimate of performance of a Mach 3 Brayton cycle (gas turbine) engine optimized for minimum fuel burned at supersonic cruise. This conceptual engine had no noise or environmental constraints imposed upon it. The purpose of these data is to define an upper boundary of the propulsion performance for a conceptual, Mach 3 commercial transport design. A comparison is presented that demonstrates the impact of the technology proposed for this conceptual engine on the weight and other characteristics of a proposed high-speed civil transport. This comparison indicates that the advanced technology turbojet engine described in this paper could reduce the gross weight of a hypothetical Mach 3 high-speed civil transport design from about 714 000 lb to about 545 000 lb. The aircraft with the baseline engine and the aircraft with the advanced technology engine are described in this paper.

Introduction

In March 1985 the Office of Science and Technology Policy published the National Aeronautical R&D Goals (ref. 1) and selected three national goals for future aeronautical research. These goals were

1. Subsonic goal: The purpose of this goal was to develop the technology required "for an entirely new generation of fuel-efficient, affordable U.S. aircraft operating in a modernized National Airspace System" to capture "the immense civil aircraft market opportunities by technologically superseding foreign competitive challenges."
2. Supersonic goal: The purpose of this goal was "to attain long-distance efficiency" by developing "pacing technologies for sustained supersonic cruise capacity" enabling "linking of the farthest reaches of the Pacific rim in four to five hours."
3. Transatmospheric goal: The purpose of this goal was "to secure future options" allowing the pursuit of "research toward capacity to routinely cruise and maneuver into and out of the atmosphere with takeoff and landing from conventional runways."

This paper will address the second goal (the supersonic goal) and, specifically, propose a propulsion system, without environmental constraint considerations, which might define an upper limit for a Mach 3 Brayton cycle engine optimized for minimum fuel burned at supersonic cruise. The performance limits as a function of Mach number were examined in reference 2. Some results of this examination are shown in figure 1, which presents the overall efficiency of the installed propulsion system as a function of Mach number. Note that at Mach 3 the projection was for an overall efficiency of approximately 50 to 58 percent. (See appendix for efficiency definitions.)

The purpose of this paper is to describe an advanced technology propulsion system for a Mach 3 supersonic cruise commercial vehicle that satisfies the installed overall efficiency goal described in figure 1. The purpose of this engine concept is to support various mission studies that examine the technical, economic, and environmental feasibility of future supersonic cruise commercial aircraft. This paper will describe the technical background for previous high-speed engine designs and the technology advances that would allow us to go from those designs to the Mach 3 engine concept described in the present paper. This proposed Mach 3 engine concept will then be described including its performance, unique features, technology level, weight and scaling laws, and overall geometry. This engine concept has been optimized for minimum fuel burned at Mach 3 and approximately 60 000 ft. The conceptual vehicle using this engine will then be described including the possible mission profiles and aircraft thrust-to-weight versus wing-loading diagrams (the so-called "thumbprint" sizing chart). Finally, environmental concerns will be briefly discussed.

Symbols

A	inlet reference area
A_o	inlet area, ft^2
C_D	drag coefficient, $\frac{D}{qS}$ for aircraft and $\frac{D}{qA_o}$ for engine
C_L	lift coefficient, $\frac{L}{qS}$
C_v	nozzle velocity coefficient, $\frac{V_{j,\text{actual}}}{V_{j,\text{ideal}}}$
D	drag, lb
d	diameter, ft
F_n	net thrust
L	lift, lb
l	length, ft
M	Mach number
P	pressure, lb/ft^2
q	dynamic pressure, lb/ft^2
S	reference area, ft^2

T	thrust, lb
V	velocity, ft/sec
W	weight, lb
w	mass flow
w_a	airflow
Δ	change in
η	efficiency

Subscripts:

a	air
ad	adiabatic
b	base
B	burner
C	compressor
c	cooling air
f	friction
j	jet
max	maximum
o	zero lift
ov	overall
poly	polytropic
R	roughness
t	turbine
T	stagnation
w	wave
∞	free stream
1	unscaled parameter
2	scaled parameter

Abbreviations:

AB	afterburner
Alt	altitude, ft
AST	advanced supersonic transport
DGW	design gross weight, lb
DW	dry weight, lb
EW	empty weight, lb
HP	high pressure
LE	leading edge
LP	low pressure
n.mi.	nautical mile
P.C.	power code, used to differentiate power levels at given Mach numbers and altitudes
OPR	overall compressor pressure ratio
SCR	Supersonic Cruise Research
SFC	specific fuel consumption, $\frac{\text{lb/hr}}{\text{lb}}$
SLS	sea level static
TE	trailing edge
TET	turbine entry temperature
VCE	variable cycle engine
ZFW	zero-fuel weight, lb

Technical Background

The British and French-designed Olympus 593 Mk 610 engine (ref. 3), which powers the Concorde, is a reasonable point of departure when considering future high-speed engines because this engine has been thoroughly tested and has been in commercial service since 1975. The Olympus 593 engine is a two-spool turbojet with partial afterburning. The maximum sea level static thrust is 37 700 lb, and the engine plus exhaust system weighs 7465 lb. The engine has a mass flow of 410 lb/sec, a turbine entry temperature of 1980°F, and a compressor pressure ratio of 15.5. The Mach 2 cruise specific fuel consumption is 1.19, which gives an overall efficiency of 41 percent. (See appendix for efficiency definitions.) An analysis of the various losses for this engine is shown in figure 2. At cruise, the compressor pressure ratio of 12.07 and the inlet pressure recovery combine to an overall engine total pressure ratio of 88.5. The ideal cycle efficiency of this engine is approximately 74 percent, the internal engine efficiency is 74 percent, and the propulsive efficiency is 74.5 percent, which combine ($0.74 \times 0.74 \times 0.745 = 0.41$) to give the 41 percent overall efficiency. This is a remarkable achievement for an engine designed in the early 1960's. It is interesting to note in figure 2 that the propulsive efficiency is one of the largest single loss mechanisms. Unfortunately, it is not practical to increase the propulsive efficiency much beyond 80 percent because as this parameter is increased, the engine net thrust approaches zero. (As the propulsive efficiency approaches 100 percent, the exhaust velocity approaches the flight velocity until, at a propulsive efficiency of 100 percent, the exhaust jet velocity and the flight velocity are equal and the engine produces no net thrust.) All other losses are approximately equal, which implies, since there are several

presented as a parameter. The goal level of 5 percent or less for the propulsion system weight fraction is a challenging but achievable goal for future development.

Advanced Mach 3 Engine Concepts

A conceptual, advanced technology two-spool turbojet engine as described below (with and without an afterburner) is proposed as a potential power plant to answer the above challenge for a high-speed propulsion system. This conceptual engine would utilize a combination of more efficient engine components, better cooling technology, and the development of advanced materials to allow the higher operational temperatures and component efficiencies required for the improved performance levels and reduced weight. This conceptual engine is close to the thermodynamic limits for the design conditions. The engine data describing this proposed concept were computed with a computer program similar to that described in reference 7. The engine was optimized for Mach 3 cruise at approximately 60 000 ft. Both the afterburning and nonafterburning engines would have the following specifications:

Technology availability date	2005–2010
Overall pressure ratio	38.6
Maximum turbine inlet temperature, °R	3 500
Cruise Mach number	3
Cruise altitude, ft	60 000
Compressor cruise adiabatic efficiency, percent	
Low rotor	87.2
High rotor	89.4
Turbine cruise adiabatic efficiency, percent	
Low rotor	89.0
High rotor	90.0
Nozzle (at cruise)	
Discharge coefficient	0.99
Velocity coefficient	0.99
Burner (at cruise)	
Total pressure drop	0.03
Combustor efficiency, percent	99.0
Inlet (at cruise)	
Total pressure recovery	0.883

The nonafterburning engine in the 383 lb/sec sea level static size has the following characteristics:

Airflow size (sea level static), lb/sec	383
Net thrust (sea level static), lb	35 667
Engine weight (bare engine), lb	2 750
Engine weight (installed), lb	4 436
Engine thrust/weight (sea level static, installed)	8.04

A schematic of the nonafterburning engine installed with a two-dimensional inlet (ref. 8) is shown as figure 10.

The afterburning engine was also in the 383 lb/sec sea level static size and has the following characteristics:

Airflow size (sea level static), lb/sec	383
Net thrust (sea level static, non AB/AB), lb	35 667/61 271
Engine weight (bare engine), lb	3 561
Engine weight (installed), lb	5 247
Engine thrust/weight (installed, non AB/AB)	6.80/11.7

A schematic of the afterburning engine concept installed with a two-dimensional inlet (ref. 8) is shown as figure 11.

The engines can be scaled by using the scaling rules outlined in table I.

The performance of these engines is summarized in figures 12–15 for the nonafterburning engine and figures 16–19 for the afterburning engine. The propulsion system drag coefficient, including both inlet and nozzle drag, is shown in figure 15 for the nonafterburning engine and in figure 19 for the afterburning engine. This drag information was computed for all power settings. The technique described in reference 9 was used to compute the installation drag coefficients. The inlet total pressure recovery used in the calculation of the performance of both engine concepts is shown in figure 20. A nozzle velocity coefficient of 0.99 and a discharge coefficient of 0.99 was used in all the calculations.

Both engines are designed to have an overall efficiency at the Mach 3 nonafterburning cruise design point of slightly over 54 percent.

The relative cruise performance of these study engines compared with other similar engines, both in-service and conceptual, can be determined by examining table II. Note that at the cruise condition the conceptual engines described in this report have a 15-percent improvement in overall efficiency over the conceptual engines used in reference 6. Note also that the conceptual engines used in reference 6 had a 13-percent advantage over the Concorde engines which are, of course, in service. The conceptual engines of reference 10 fall in between the engines of reference 11 and the engines described in this report. In the following section, the conceptual engine of this paper will be installed in the aircraft concept of reference 10 and compared with the aircraft/engine combination of reference 10.

Advanced Mach 3 Baseline Aircraft Concept

Configuration Description

The advanced Mach 3 baseline configuration (ref. 10) is a blended wing/body concept with a modified platypus nose (see fig. 21). The main cabin section is configured for 250 passengers (fig. 22). Six engines are mounted in the nacelles, with three engines per pod on the wing lower surface adjacent to the fuselage. Each engine's thrust-vectoring nozzle extends aft of the wing trailing edge. Fuel is contained in integral wing tanks and in three fuselage mounted tanks. The aft fuselage tanks are used also for aircraft center-of-gravity control. The remaining subsystems, including environmental control, hydraulic, electrical, auxiliary power, and engine-driven accessories, are mounted in the fuselage below the cabin floor between the wing rear spar and aft fuselage fuel tank.

Mass Properties

An estimate of the conceptual aircraft weight and balance is described in reference 10. The results of these calculations are summarized in table III and figure 23. The technology level assumed for these estimates is compatible with year 1995 technology readiness and is described in detail in reference 10. The fuselage is assumed to be constructed of super-plastic-formed, diffusion-bonded titanium. Wing structure, including fairings, control surfaces, and fuel tanks, is assumed to be made of composite materials such as graphite or Kevlar fiber and epoxy. On the landing gear, radial tires are used with lightweight forged wheels and carbon brakes. In general, this technology represents a 15- to 20-percent reduction in weight relative to current structure and systems.

Configuration Aerodynamics

The technique for estimating the vehicle aerodynamics is described in detail in reference 10. The zero-lift drag coefficient as a function of flight Mach number for the configuration is shown in figure 24, where for computational purposes the skin friction drag coefficient is based on an altitude of 40 000 ft. Supersonic and subsonic drag polars are shown in figures 25 and 26, respectively.

Maximum lift-to-drag ratios varied from about 14 at high subsonic speed to 9.4 at Mach 3 (fig. 27). Much more detail on the aerodynamic characteristics of the baseline configuration is presented in reference 10.

Mission Description

The mission chosen is 6500 nautical miles long and would represent more than 90 percent of the long-range market routes of interest. A summary of parameters describing the mission is shown in table IV. The baseline aircraft instantaneous weight as a function of mission range is shown in figure 28.

Typical Sizing and Performance Trade-Offs

During the conceptual design process, the engine characteristics and vehicle aerodynamic characteristics are determined for the vehicle. These characteristics are then scaled by using the vehicle thrust-to-weight ratio as an independent parameter to scale the engine and the vehicle wing loading to scale the vehicle aerodynamics. The purpose of this scaling is to achieve an optimum vehicle for a particular mission. The chart which graphically demonstrates this optimization process is sometimes called a "thumbprint" chart. The sizing chart or thumbprint for the nonafterburning turbojet engine of this paper installed on the advanced commercial transport concept described previously is shown as figure 29. In this figure, the maximum dry sea level static thrust-to-weight ratio and wing loading are the independent variables (i.e., Y-axis and X-axis, respectively), and lines of constant aircraft gross weight are shown as a parameter. The takeoff field length and approach speed are also shown in this chart and are used as constraints to define areas of the chart where designs are impractical. For example, if it is desirable to have a vehicle takeoff in 10 000 feet or less and have an approach speed of no more than 150 knots, then the vehicle gross weight can be in the center of the thumbprint or somewhat less than 545 000 pounds.

The thumbprint for the afterburning turbojet described above using the same aerodynamic configuration is shown in figure 30. If the same constraints are used, the afterburning turbojet configuration is predicted to weigh about 575 000 lb. Thus, for the chosen constraints, the afterburning turbojet configuration would have a gross weight about 30 000 lb heavier than for the nonafterburning turbojet configuration. An examination of the climb thrust available for the afterburning and nonafterburning configurations (fig. 31) and the climb thrust used for both configurations (fig. 32) indicates that the afterburning configuration has considerable excess thrust during climb compared with the nonafterburning configuration. However, when the minimum fuel climb optimization is performed, most of this excess thrust is not used (fig. 32). Thus, the extra weight of the afterburner is not offset by a fuel savings and is, therefore, not an advantage. It should be noted that

References

1. *National Aeronautical R&D Goals—Technology for America's Future.* Executive Office of the President, Office of Science and Technology Policy, Mar. 1985.
2. *Aeropropulsion '87, Session 6—High-Speed Propulsion Technology.* NASA CP-10003, 1987.
3. Taylor, John W. R., ed.: *Jane's All the World's Aircraft 1977–78.* Jane's Yearbooks (London).
4. *USAF Propulsion Characteristics Summary (Airbreathing).* Air Force Guide No. 3, Gray Book Volume 1 (Addendum 15), U.S. Air Force, July 1988.
5. Hoffman, Sherwood: *Bibliography of Supersonic Cruise Research (SCR) Program From 1980 to 1983.* NASA RP-1117, 1984.
6. Molloy, John K.; Grantham, William D.; and Neubauer, Milton J., Jr.: *Noise and Economic Characteristics of an Advanced Blended Supersonic Transport Concept.* NASA TP-2073, 1982.
7. Fishbach, Laurence H.; and Caddy, Michael J.: *NNEP—The Navy NASA Engine Program.* NASA TM X-71857, 1975.
8. Ball, W. H.: *Rapid Evaluation of Propulsion System Effects. Volume IV—Library of Configurations and Performance Maps.* AFFDL-TR-78-91, Vol. IV, U.S. Air Force, July 1978.
9. Morris, Shelby J., Jr.; Nelms, Walter P., Jr.; and Bailey, Rodney O.: *A Simplified Analysis of Propulsion Installation Losses for Computerized Aircraft Design.* NASA TM X-73136, 1976.
10. Robins, A. Warner; Dollyhigh, Samuel M.; Beissner, Fred L., Jr.; Geiselhart, Karl; Martin, Glenn L.; Shields, E. W.; Swanson, E. E.; Coen, Peter G.; and Morris, Shelby J., Jr.: *Concept Development of a Mach 3.0 High-Speed Civil Transport.* NASA TM-4058, 1988.
11. Schweiger, F. A.: *Revolutionary Opportunities for Materials and Structures Study.* NASA CR-179642, 1987.
12. Morris, Shelby J., Jr.; Strack, William C.; and Weidner, John P.: Propulsion System Issues for the High-Speed Civil Transport Study. AIAA-87-2938, Sept. 1987.
13. *Aircraft Engine Emissions.* NASA CP-2021, 1977.
14. Shepherd, Dennis G.: *Aerospace Propulsion.* American Elsevier Publ. Co., 1972.

Table I. Scaling Rules

Weight:

$$w_2 = w_1 \times \left[\frac{w_{a,2}}{w_{a,1}}\right]^{1.12}$$

Diameter:

$$d_2 = d_1 \times \left[\frac{w_{a,2}}{w_{a,1}}\right]^{0.5}$$

Length:

$$l_2 = l_1 \times \left[\frac{w_{a,2}}{w_{a,1}}\right]^{0.5}$$

Table II. Engine Comparison

	Concorde Olympus	AST-205 (ref. 6)	ROMS (ref. 11)	Mach 3 engine (ref. 10)	Conceptual non AB	Conceptual with AB
Weight, lb (engine + nozzle)	7465	7974	7830	8444	2750	3561
Cruise:						
Mach No.	2.00	2.62	2.62	3.00	3.00	3.00
Altitude, ft	53000	60000	60000	65000	60000	60000
F_n, lb	10030	10000	17461	20121	18211	45967/18211†
F_n/W (engine + nozzle)	1.34	1.25	2.23	2.38	6.62	12.9/5.11†
Efficiency	0.41	0.47	0.51	0.50	0.54	0.33/0.54†
Percent improvement	−13	0 (base)	+8.5	+6.4	+15	−30/+15†
SLS:						
F_n, lb	38900	47500	47500	61271	35667	61271/35667†
F_n/W (engine + nozzle)	5.21	3.41	6.07	7.26	13.0	17.2/10.0†
Cruise:						
OPR	15.5	5.4	16.2	13.5	15.0	15.0
TET, °F	1970	2703	4079		3040	3040

†AB on/AB off.

Table IV. Mission Summary for the Conceptual High-Speed Civil Transport

Segment	Initial weight, lb	Fuel, lb		Time, min		Distance, n.mi.		Mach number		Altitude, ft	
		Segment	Total	Segment	Total	Segment	Total	Start	End	Start	End
Taxi out	713 696	3 697	3 697	10.0	10.0						
Takeoff	709 999	2 542	6 239	.7	10.7				.300		0
Climb	707 457	52 773	59 012	11.5	22.2	186.1	186.1	0.300	3.000	0	65 671
Cruise	654 685	264 534	323 545	203.7	225.9	5959.4	6145.4	3.000	3.000	65 671	70 000
Descent	390 151	9 772	333 318	35.3	261.1	354.6	6500.0	3.000	.300	70 000	0
Reserves	380 378	52 585	385 903								
Taxi in		1 849		5.0	266.1						
Zero fuel	327 793										

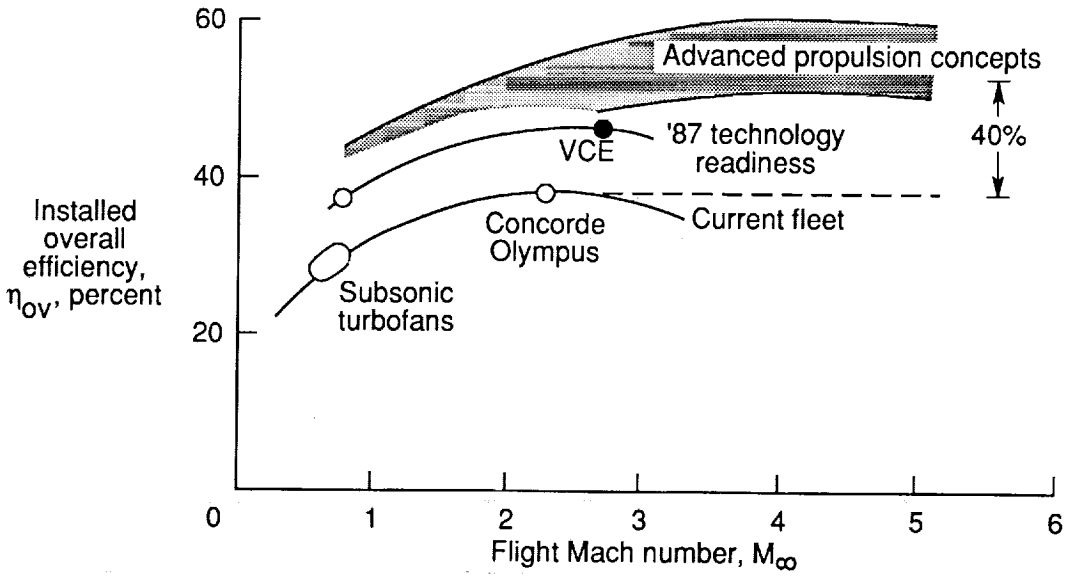

Figure 1. Propulsion system overall efficiency versus Mach number.

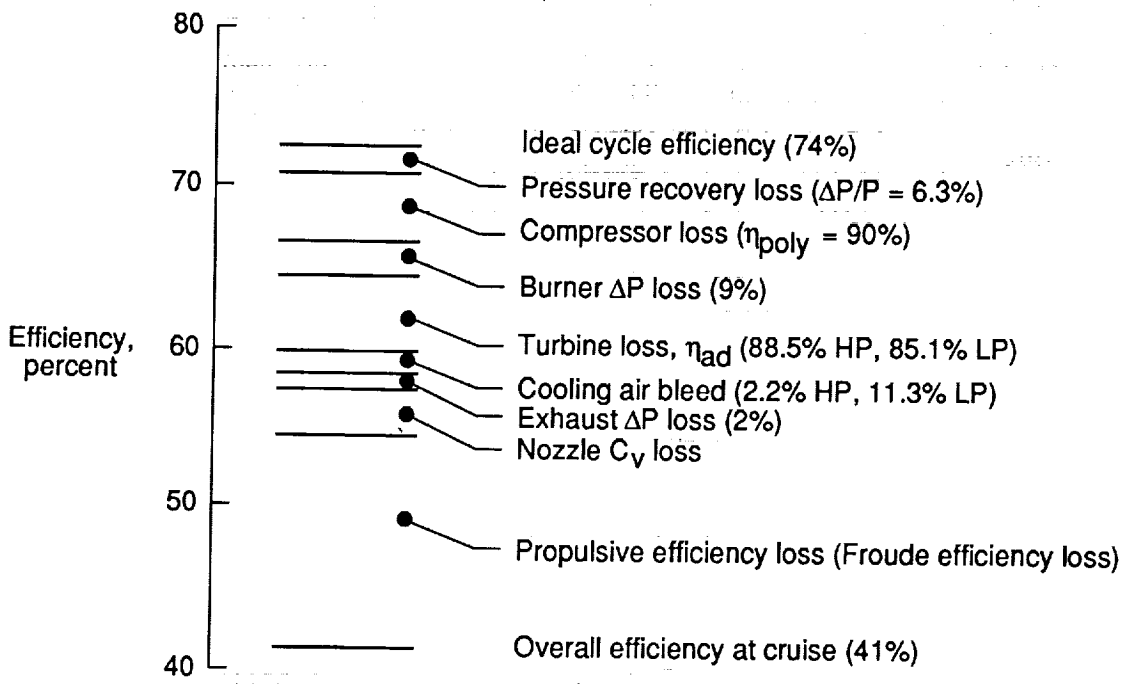

Figure 2. Estimated Concorde cruise propulsion-related efficiency losses at $M = 2$ and an altitude of 53 000 ft.

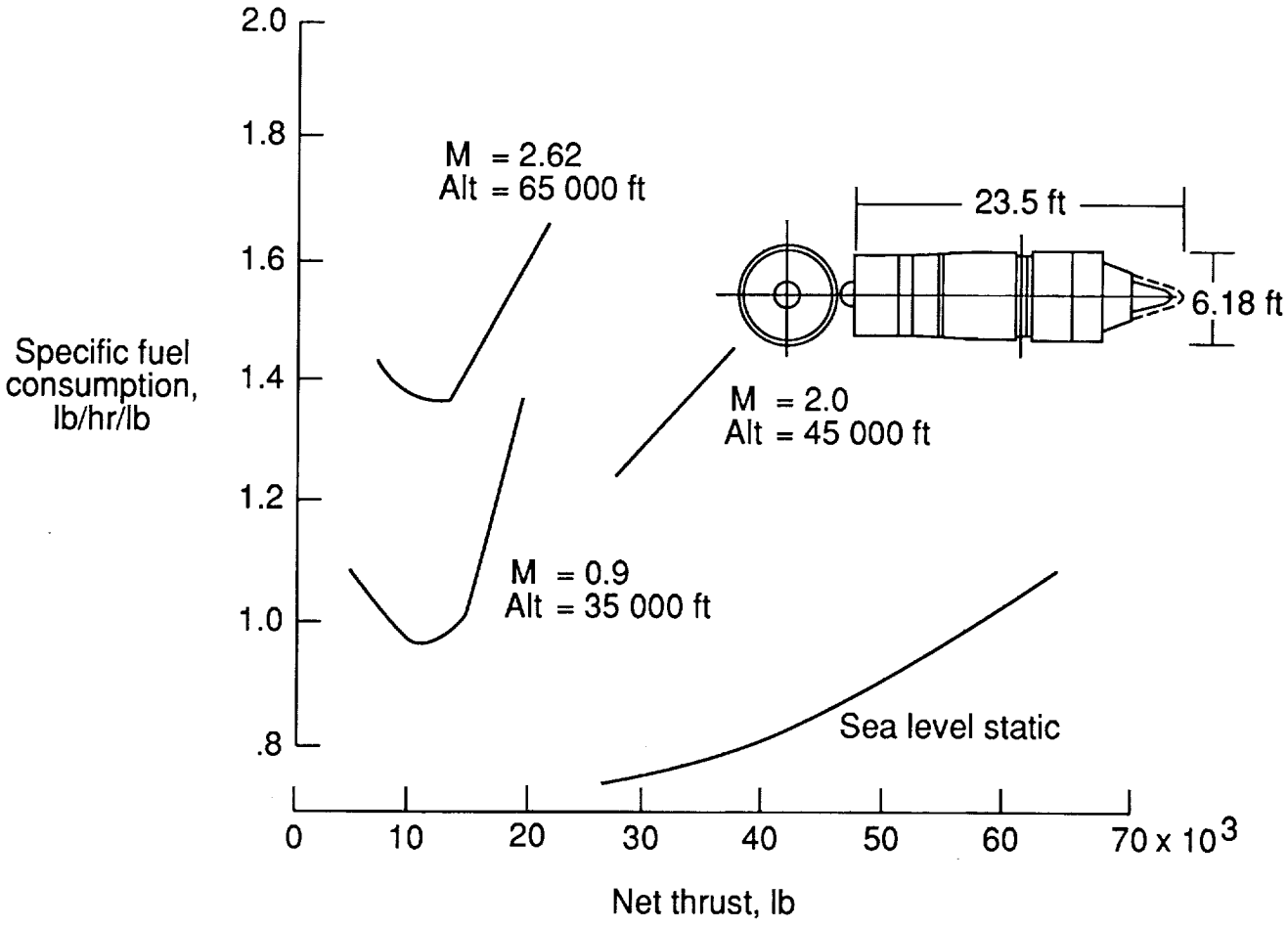

Figure 3. Engine performance for the AST-205 engine (the GE21/J11B14).

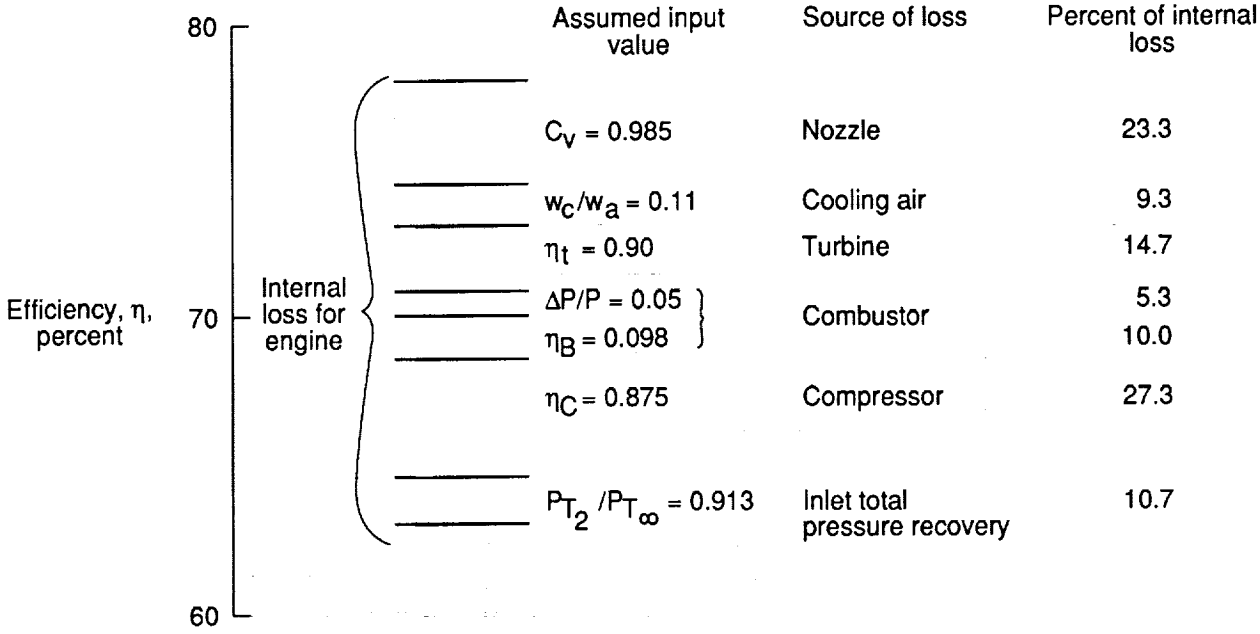

Figure 4. Estimated AST-205 cruise propulsion-related internal efficiency losses at $M = 2.7$.

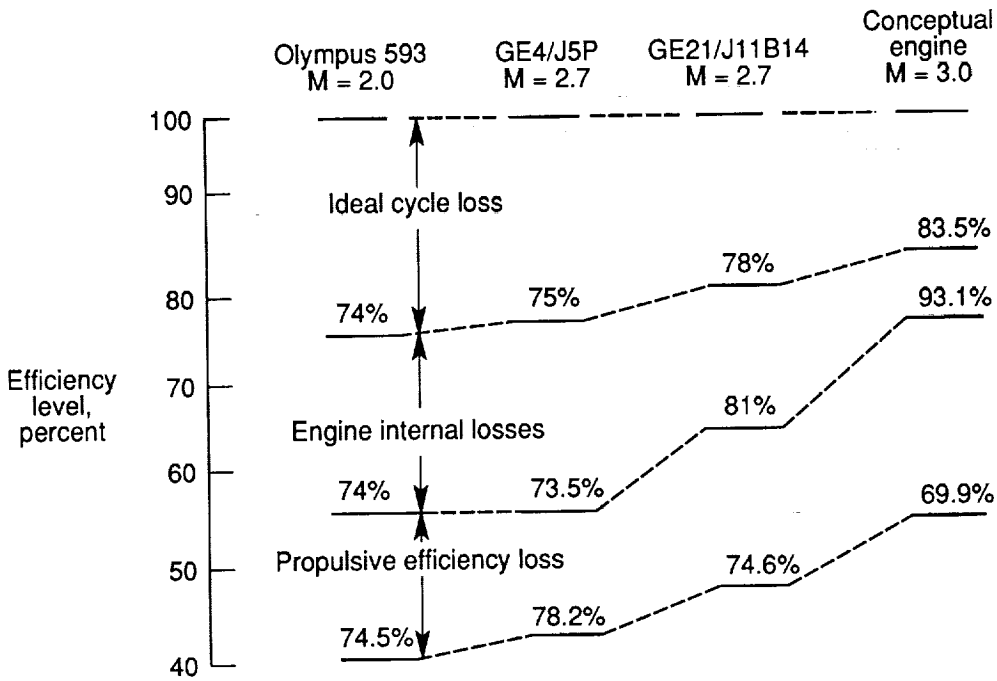

Figure 5. Comparison of the propulsion-related cruise efficiencies for engines for the Concorde, the Boeing 2707-300, the AST-205, and a conceptual engine for the present paper.

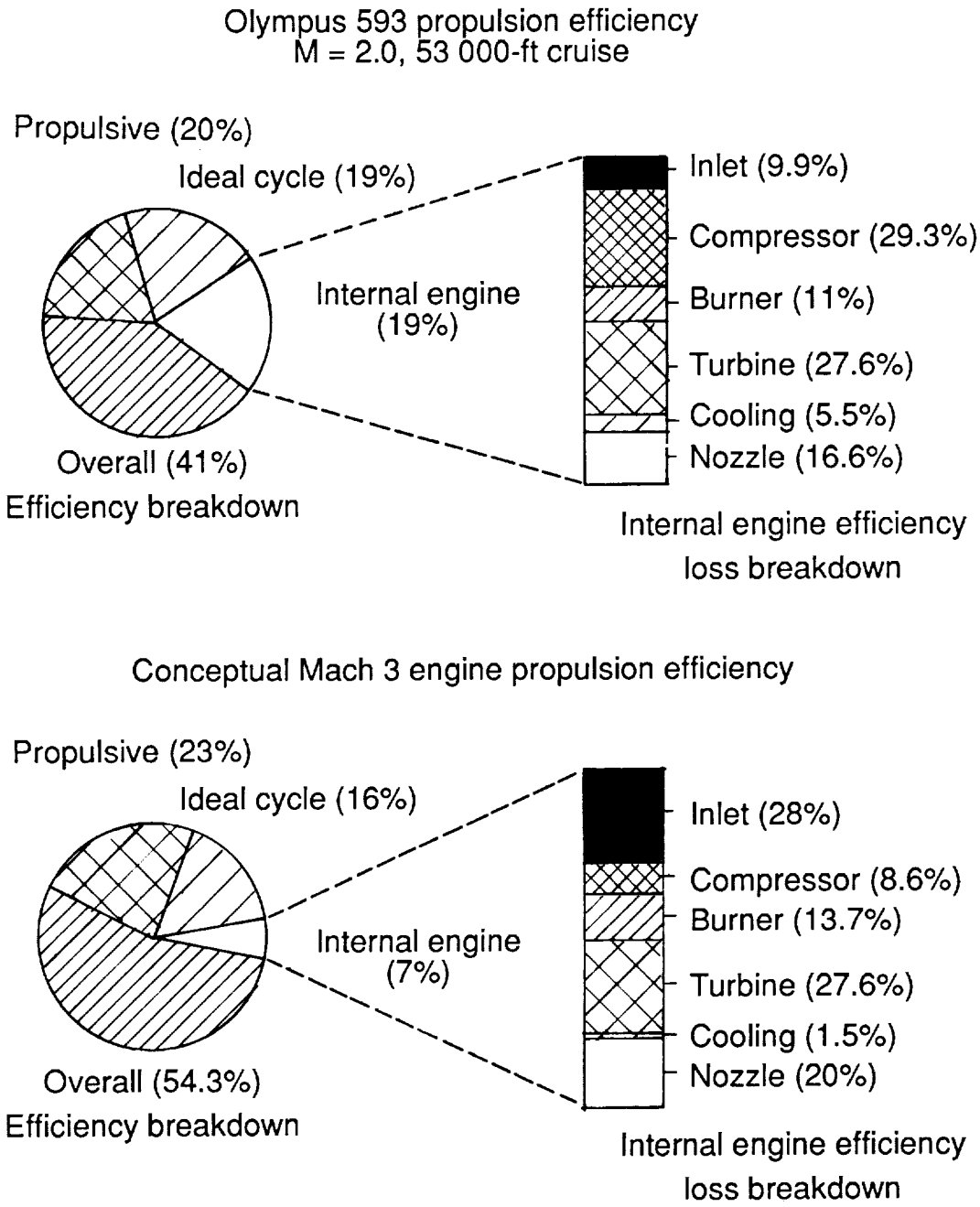

Figure 6. Propulsion-related efficiencies and engine internal efficiency losses for the Olympus engine and the Mach 3 cruise engine of this paper.

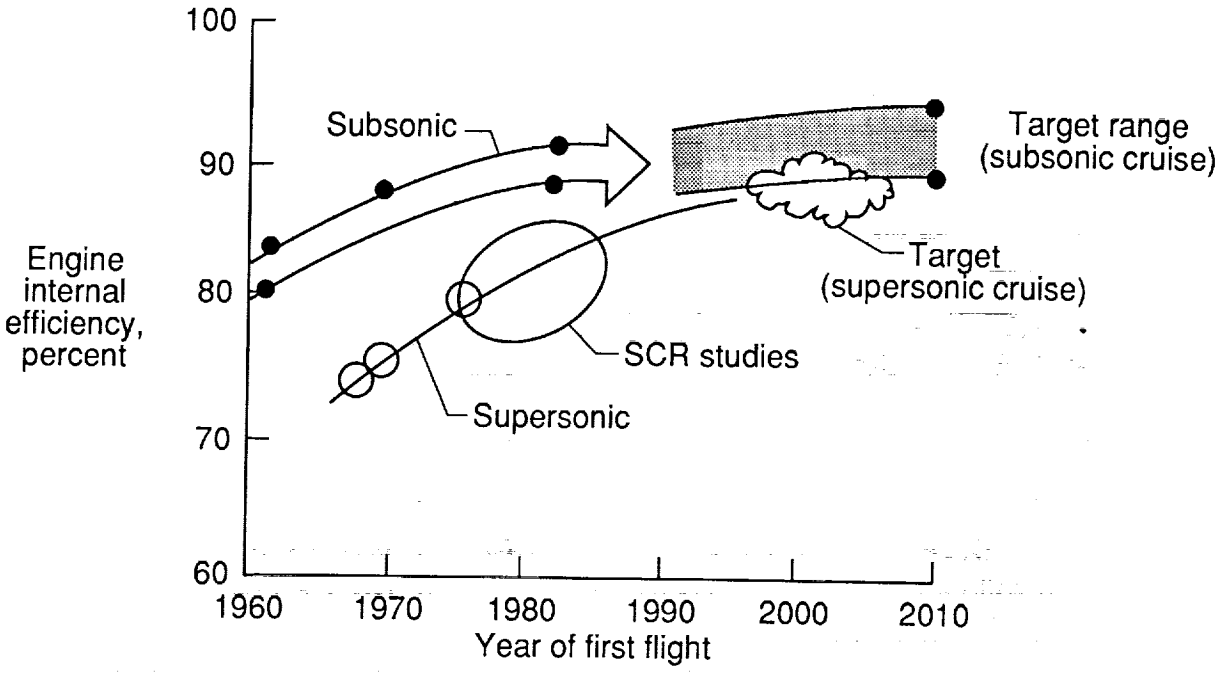

Figure 7. Trend of the internal efficiency of subsonic and supersonic engines as a function of time.

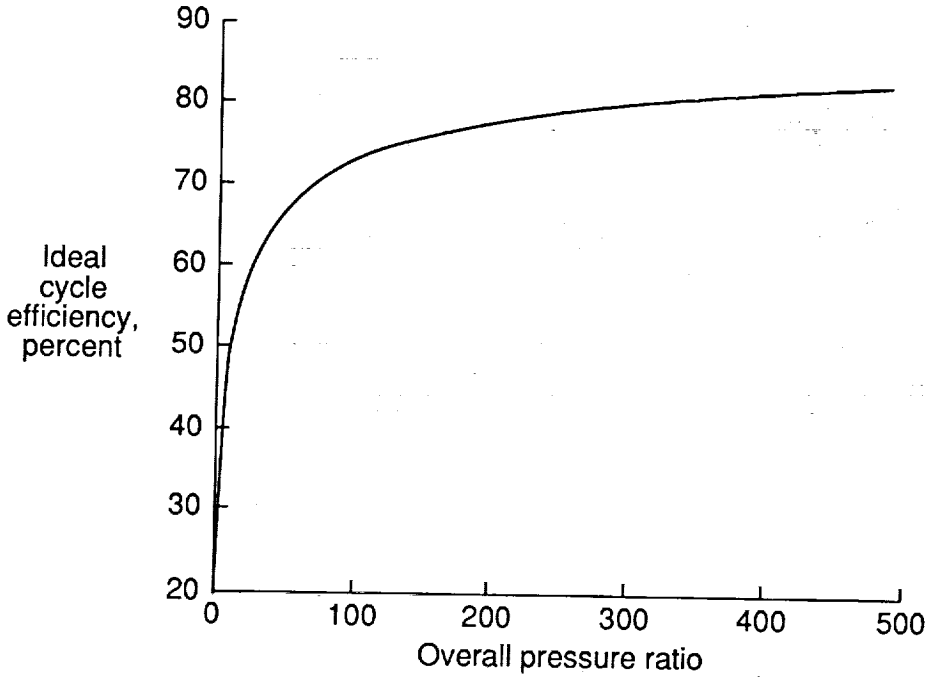

Figure 8. Ideal cycle efficiency as a function of overall engine pressure ratio.

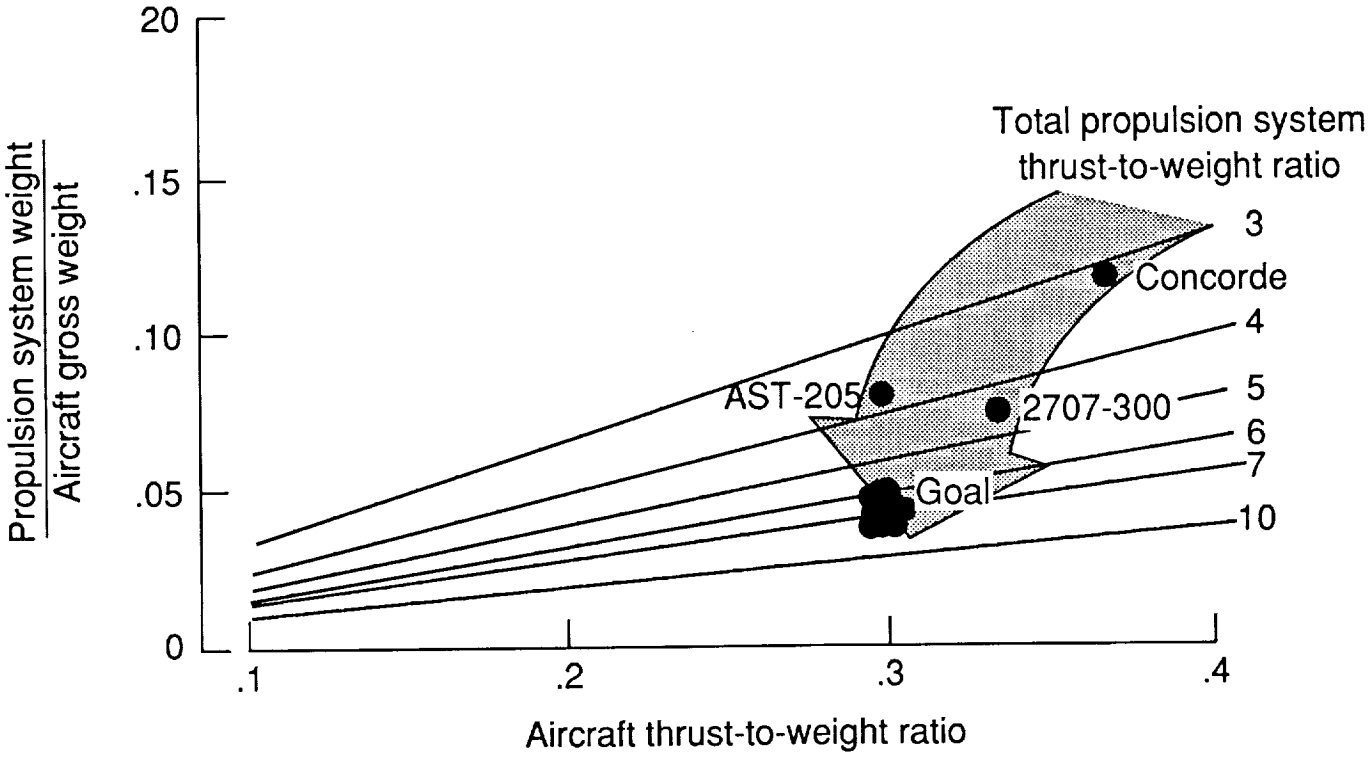

Figure 9. Factors affecting the propulsion system weight fraction of selected high-speed aircraft.

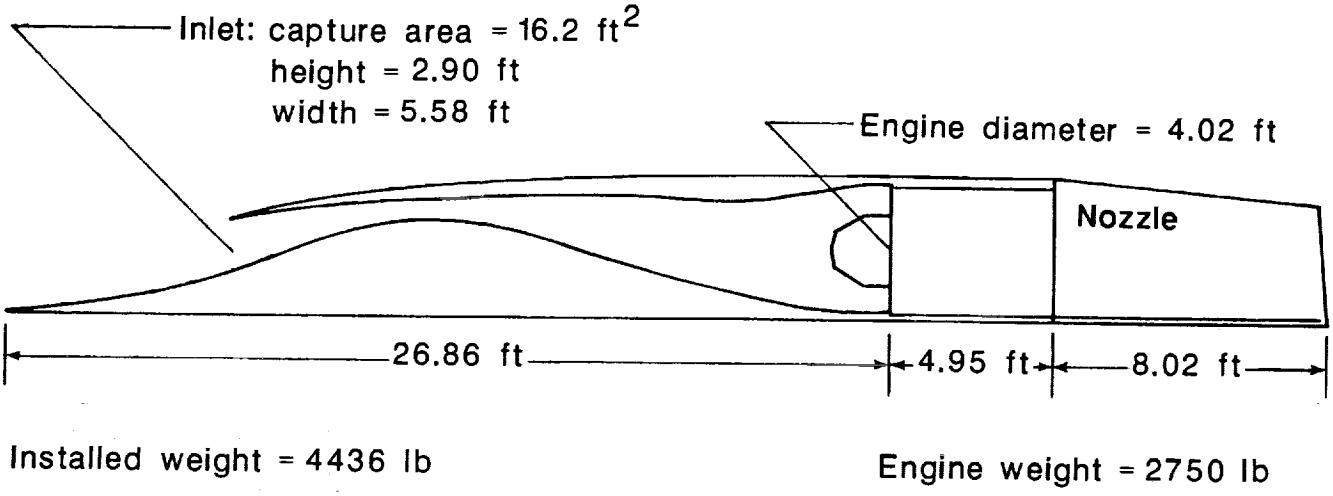

Figure 10. Schematic of nonafterburning conceptual turbojet installed in a two-dimensional inlet design.

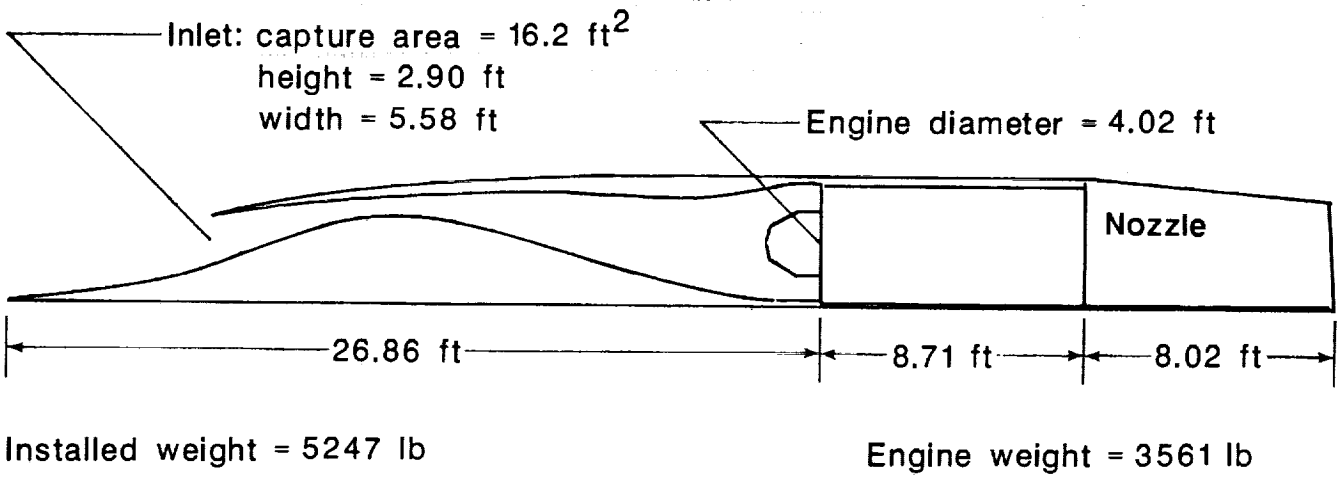

Figure 11. Schematic of afterburning conceptual turbojet installed in a two-dimensional inlet design.

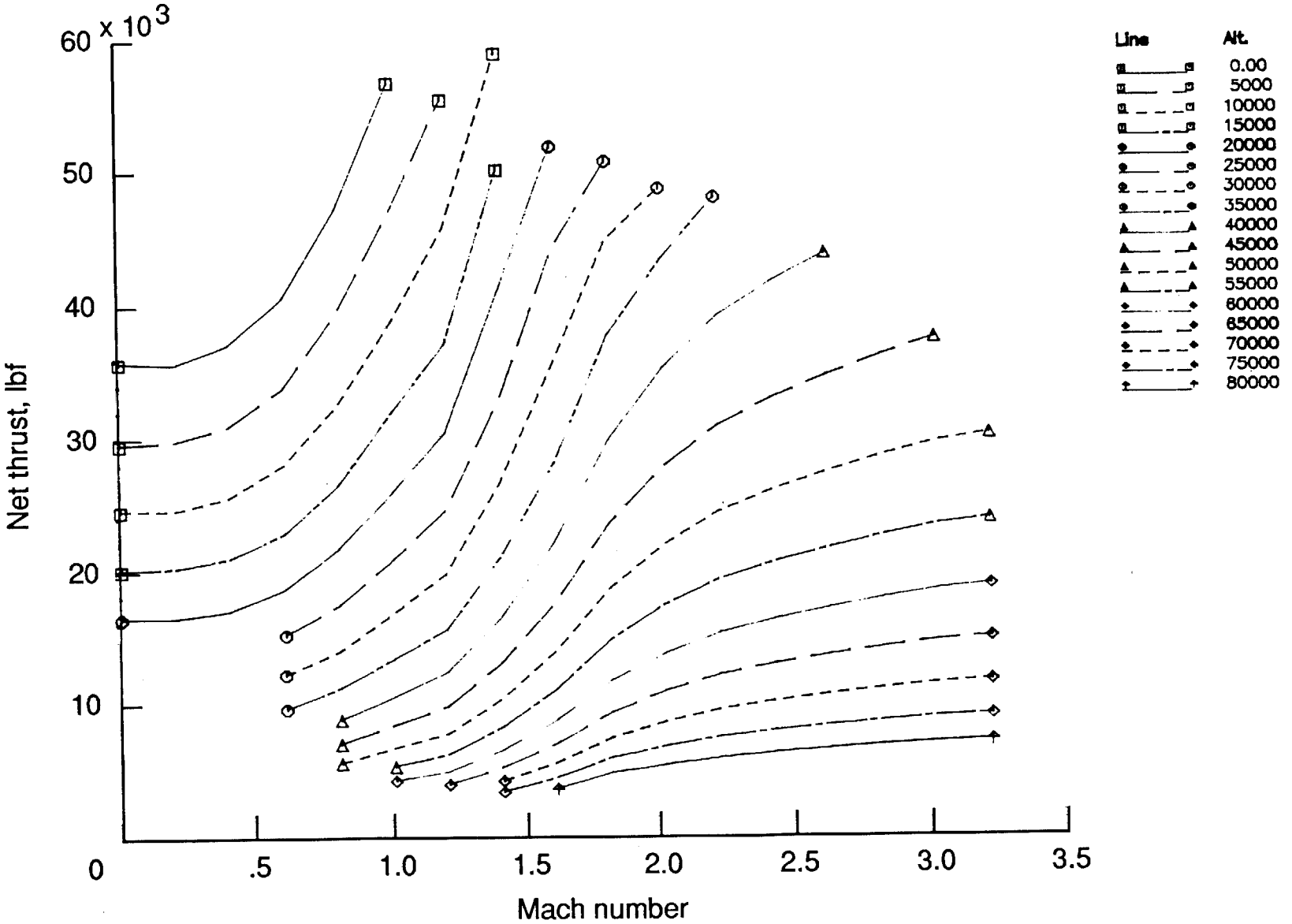

Figure 12. Net thrust versus Mach number for various altitudes for nonafterburning conceptual turbojet (maximum power condition).

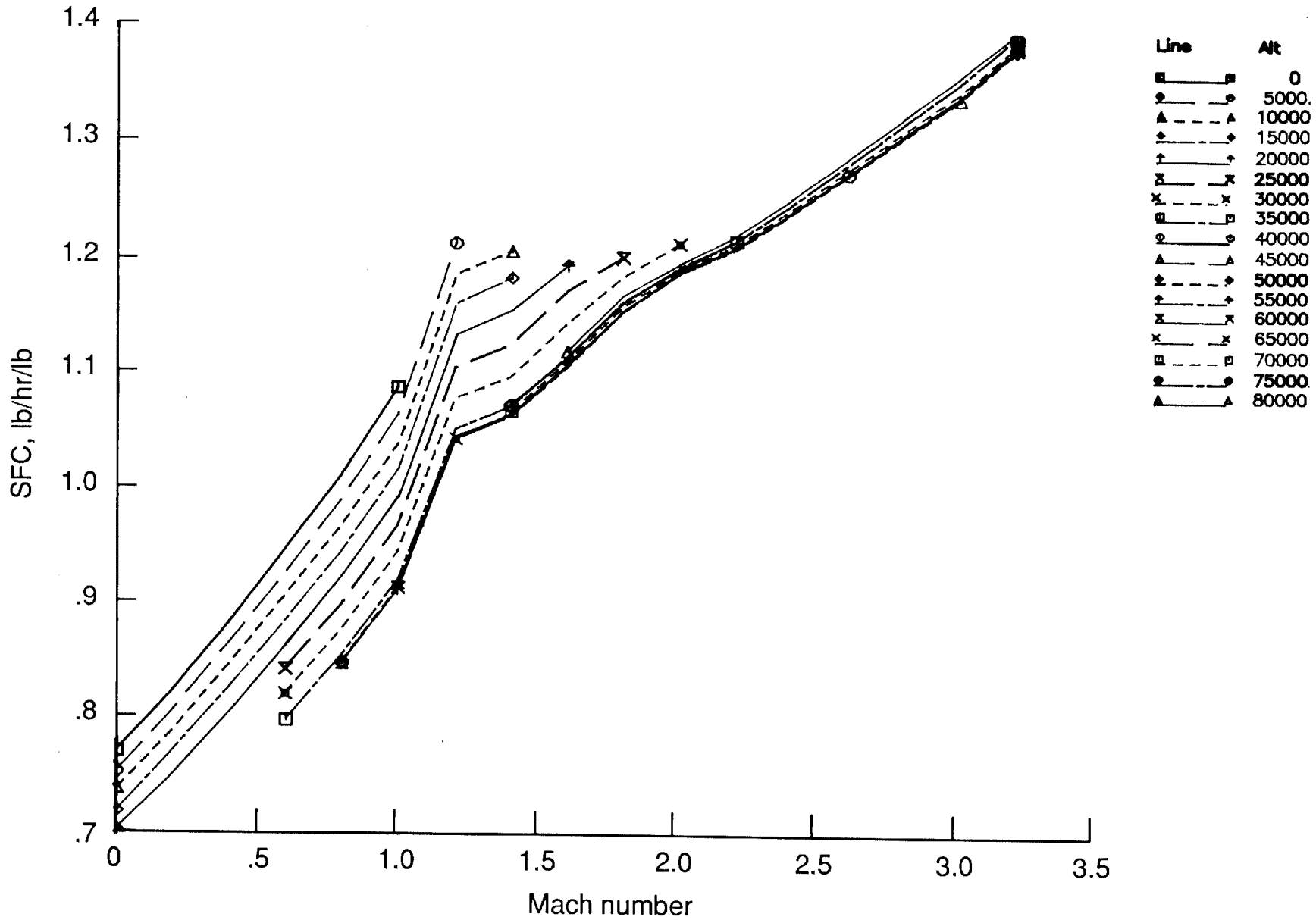

Figure 13. Specific fuel consumption (SFC) versus Mach number for various altitudes for conceptual nonafterburning turbojet (maximum power condition).

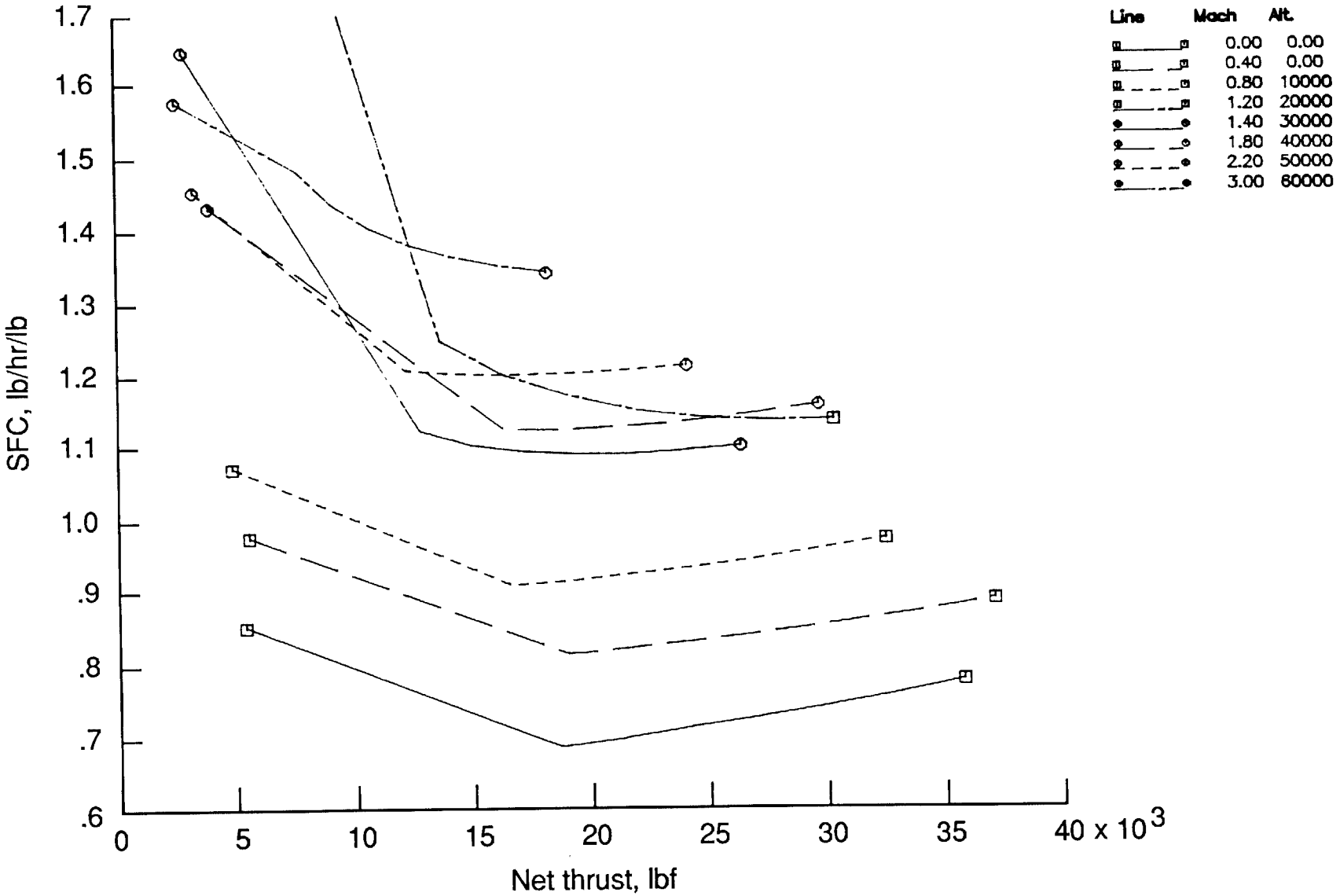

Figure 14. Specific fuel consumption (SFC) versus net thrust for various Mach number and altitude combinations for conceptual nonafterburning turbojet.

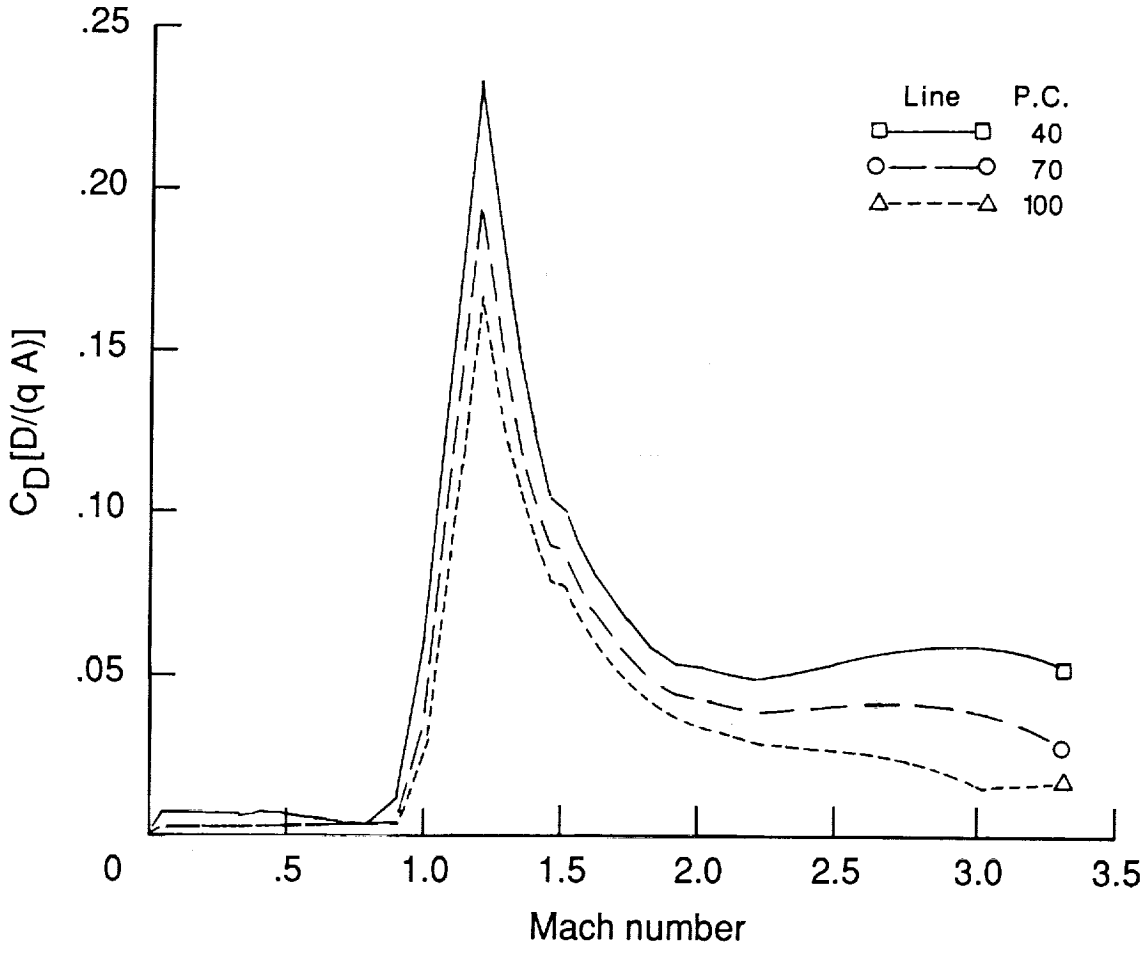

Figure 15. Propulsion system drag coefficient versus Mach number for the conceptual nonafterburning turbojet.

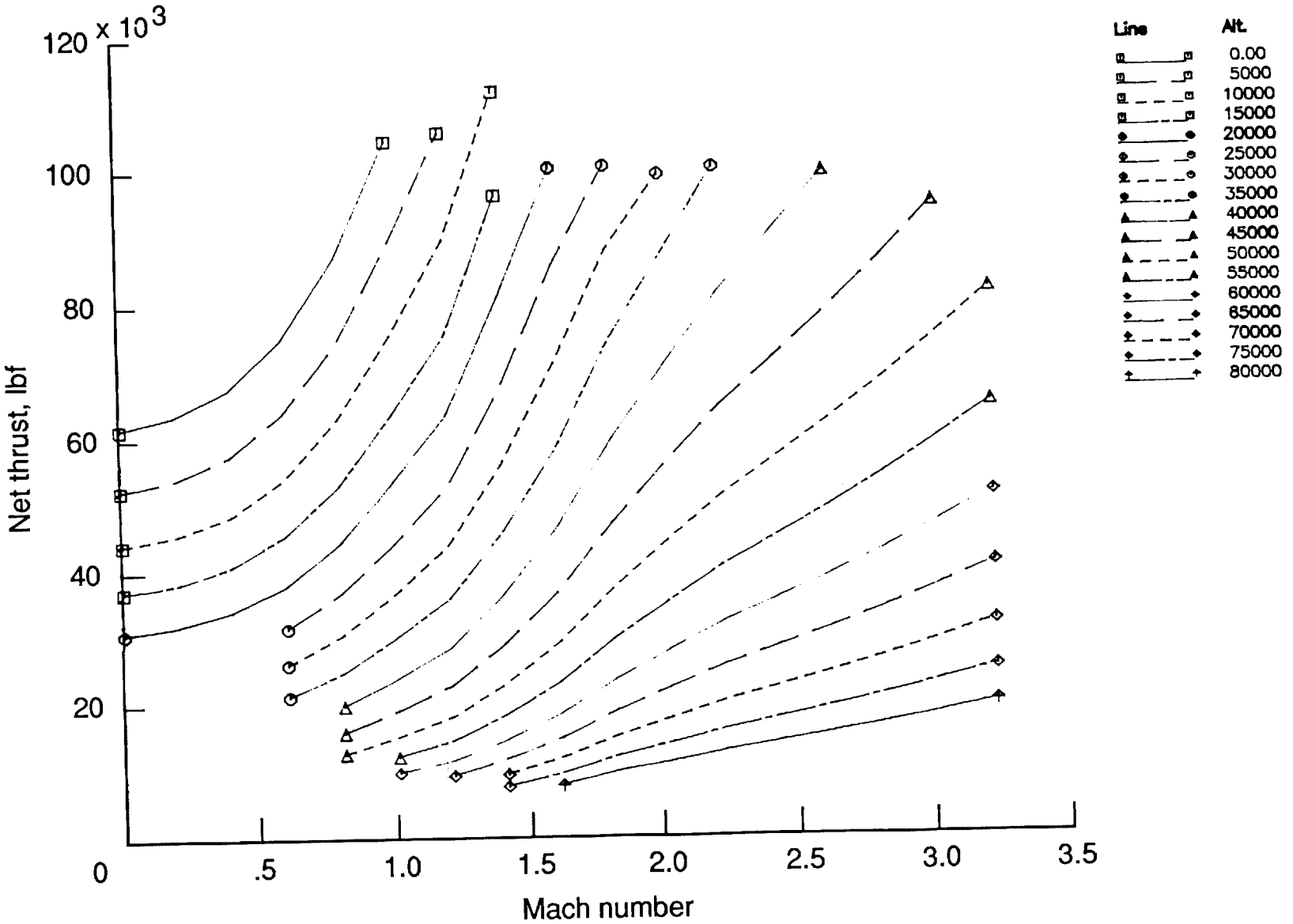

Figure 16. Net thrust versus Mach number for various altitudes for afterburning conceptual turbojet (maximum power condition).

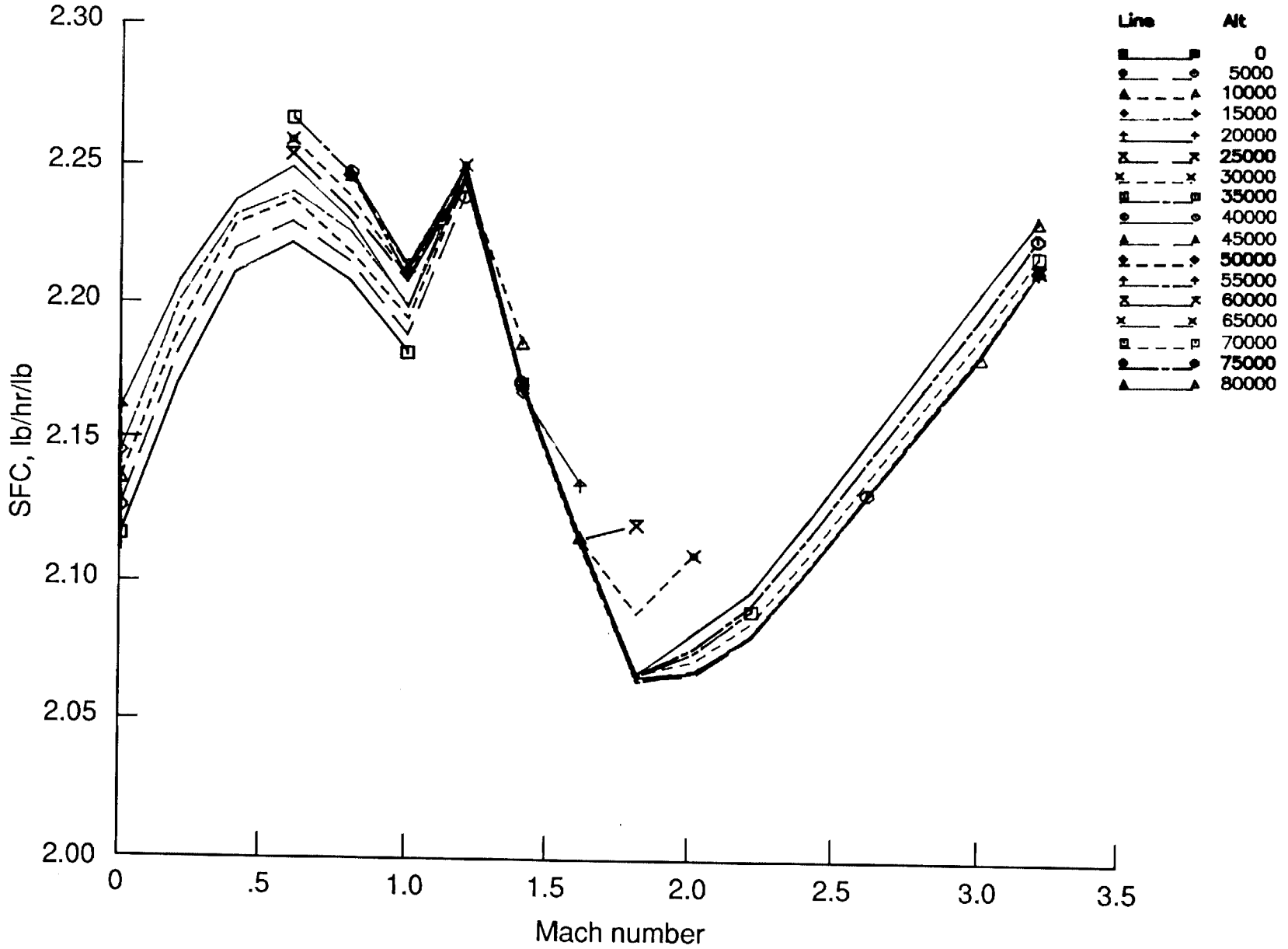

Figure 17. Specific fuel consumption (SFC) versus Mach number for various altitudes for conceptual afterburning turbojet (maximum power condition).

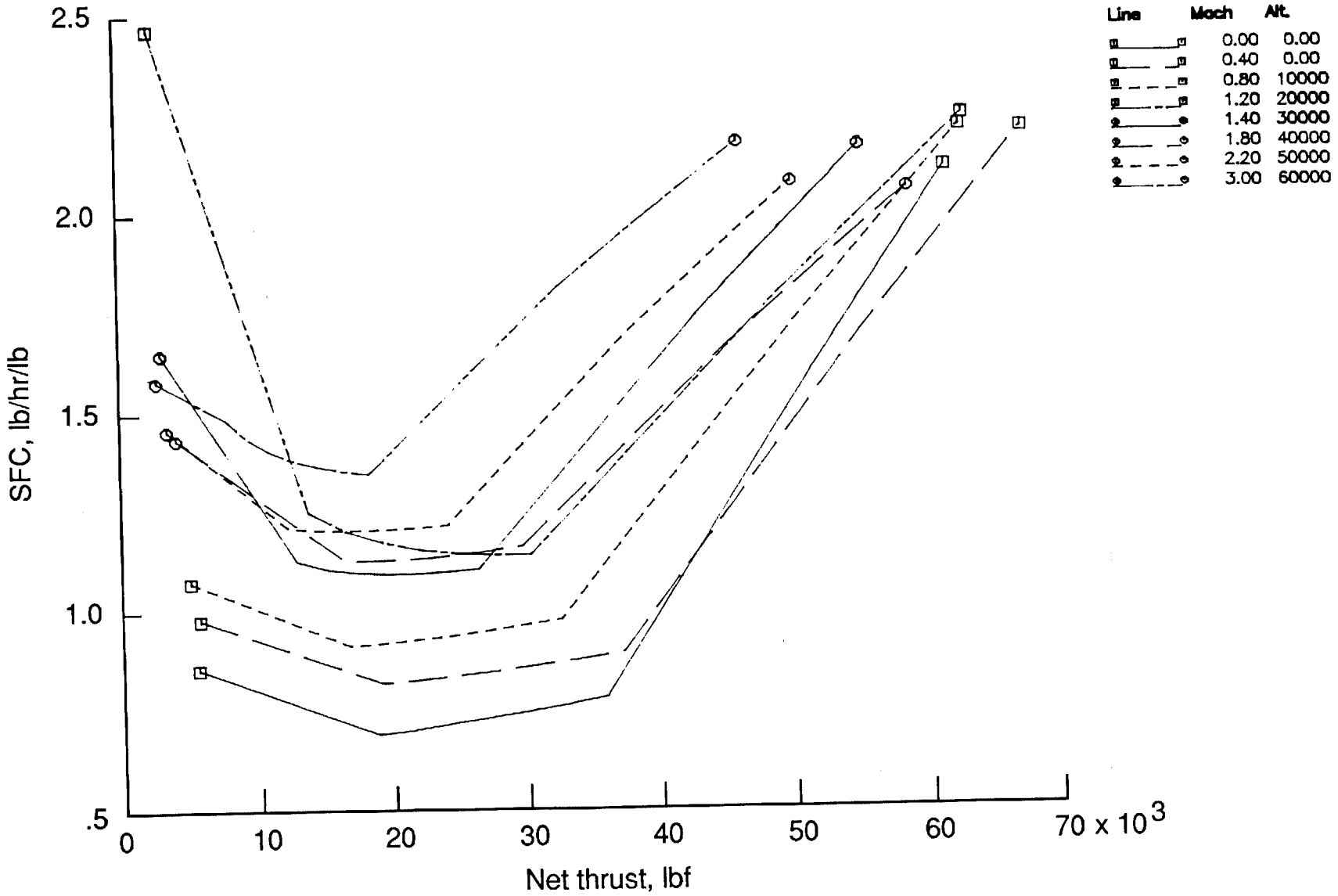

Figure 18. Specific fuel consumption (SFC) versus net thrust for various Mach number and altitude combinations for conceptual afterburning turbojet.

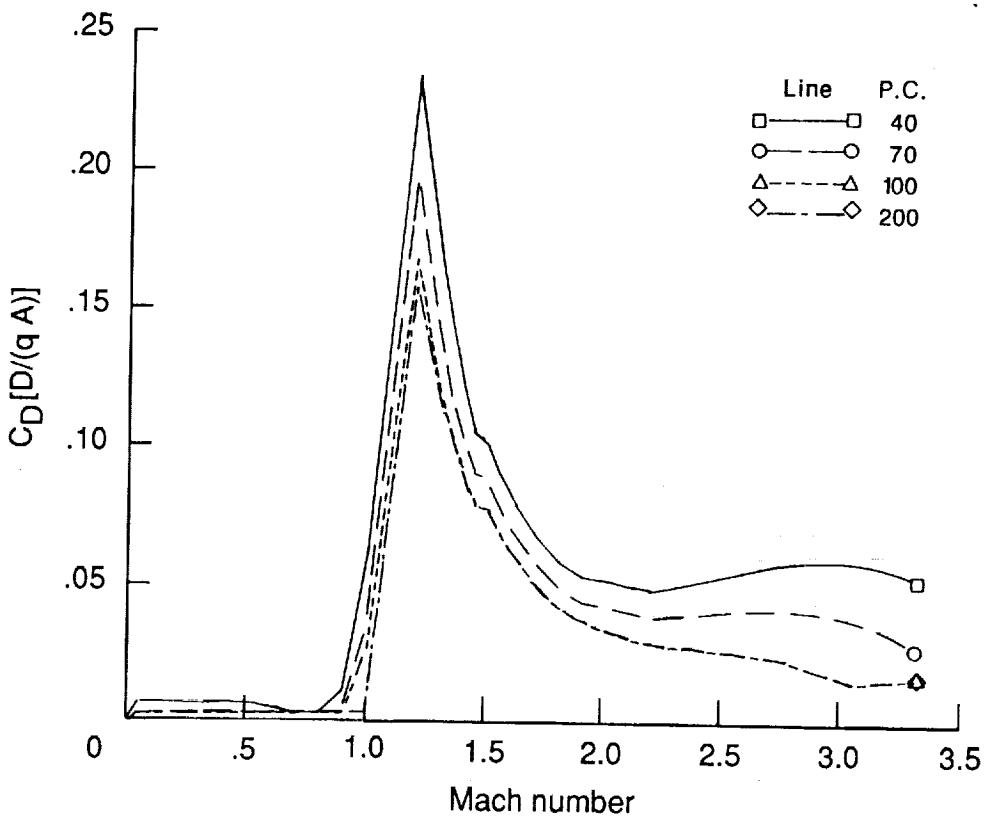

Figure 19. Propulsion system drag coefficient versus Mach number for the conceptual afterburning turbojet.

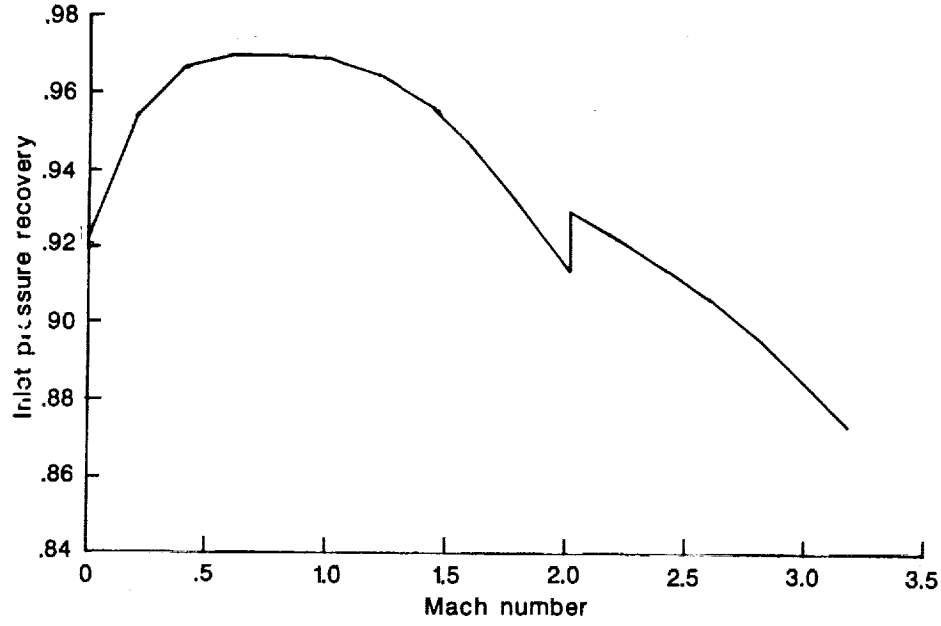

Figure 20. Inlet total pressure recovery as a function of Mach number.

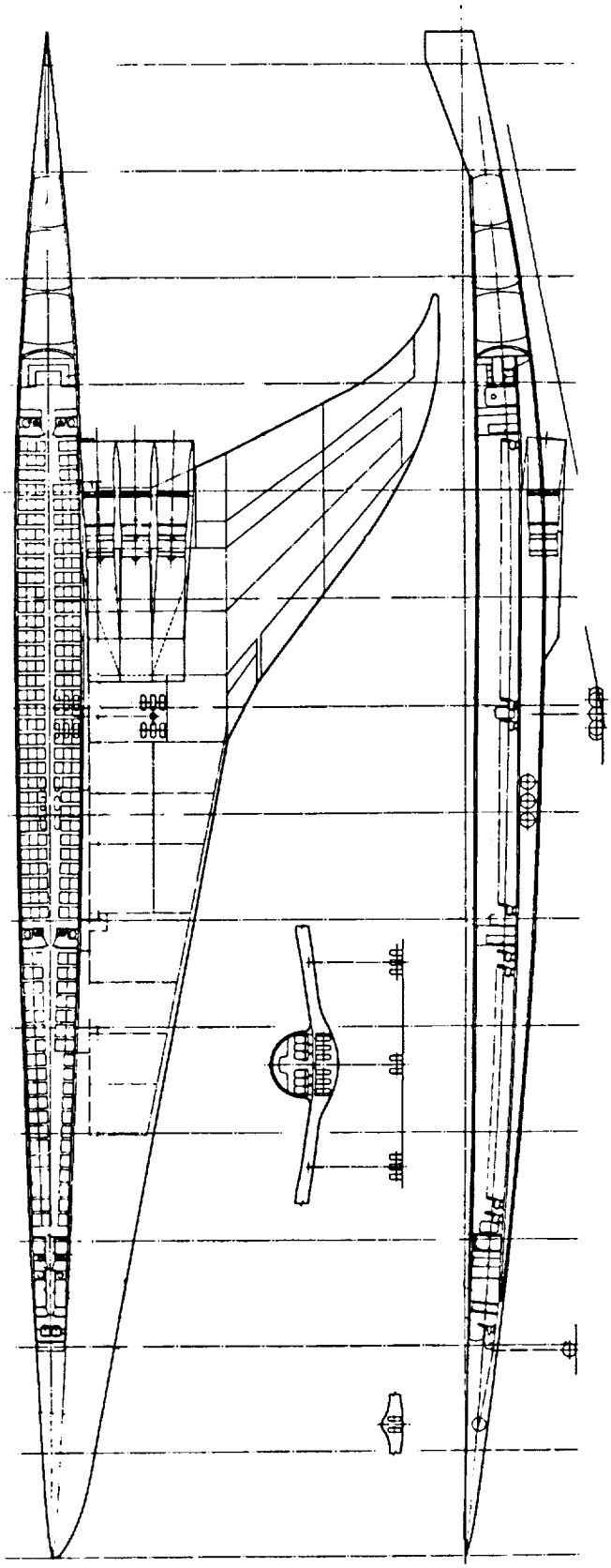

Figure 22. Inboard views.

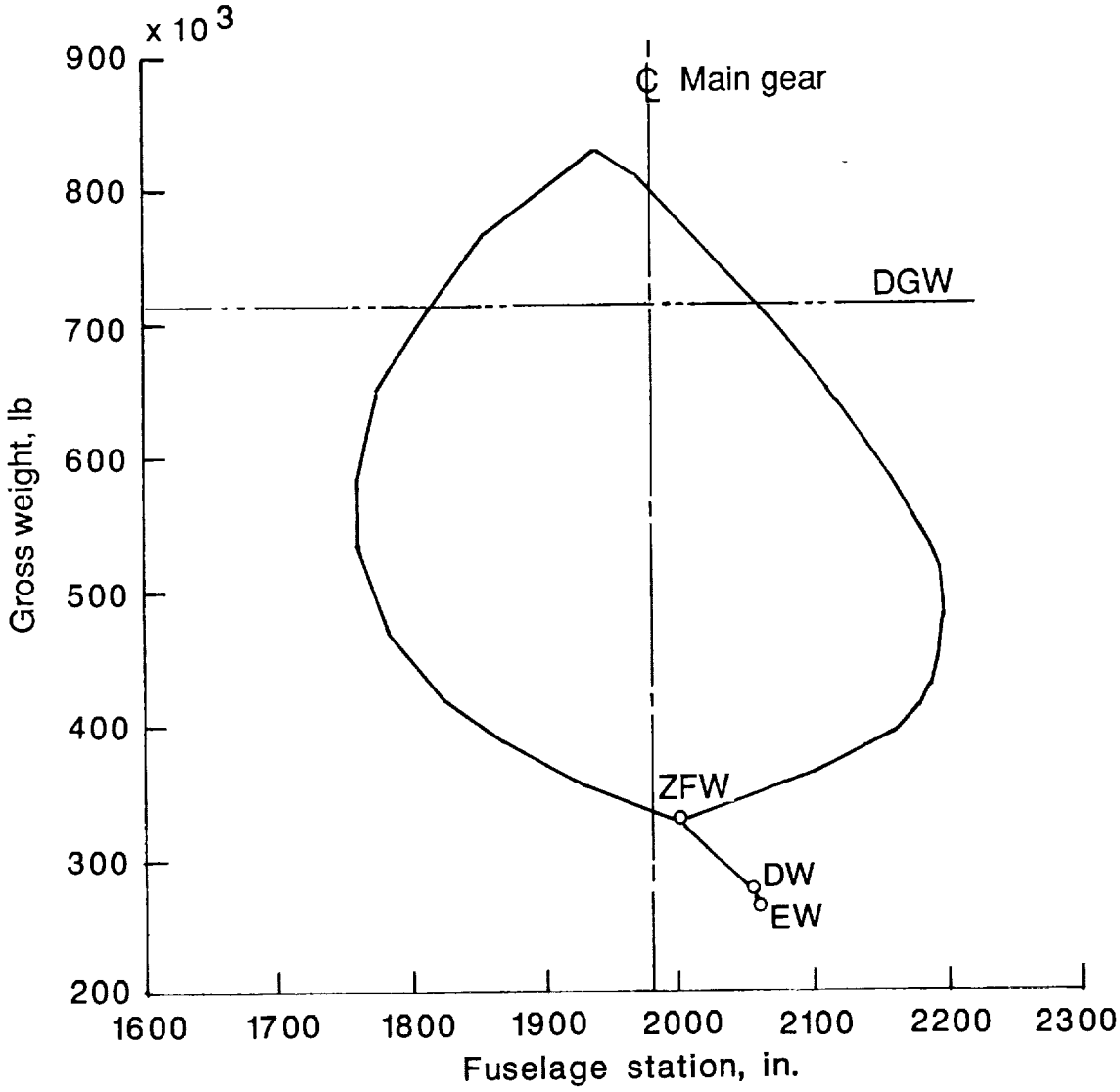

Figure 23. Baseline aircraft weight and balance diagram.

PAGE 30 INTENTIONALLY BLANK

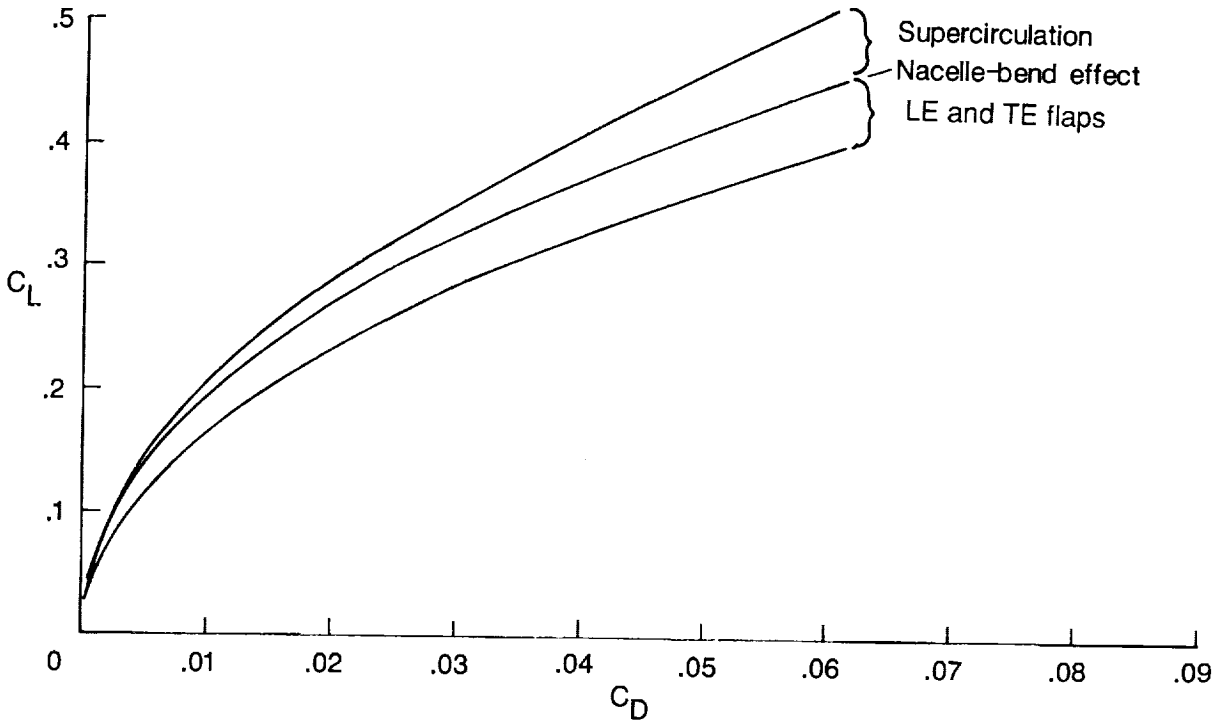

Figure 26. Typical subsonic lift coefficient versus drag coefficient for baseline aircraft concept.

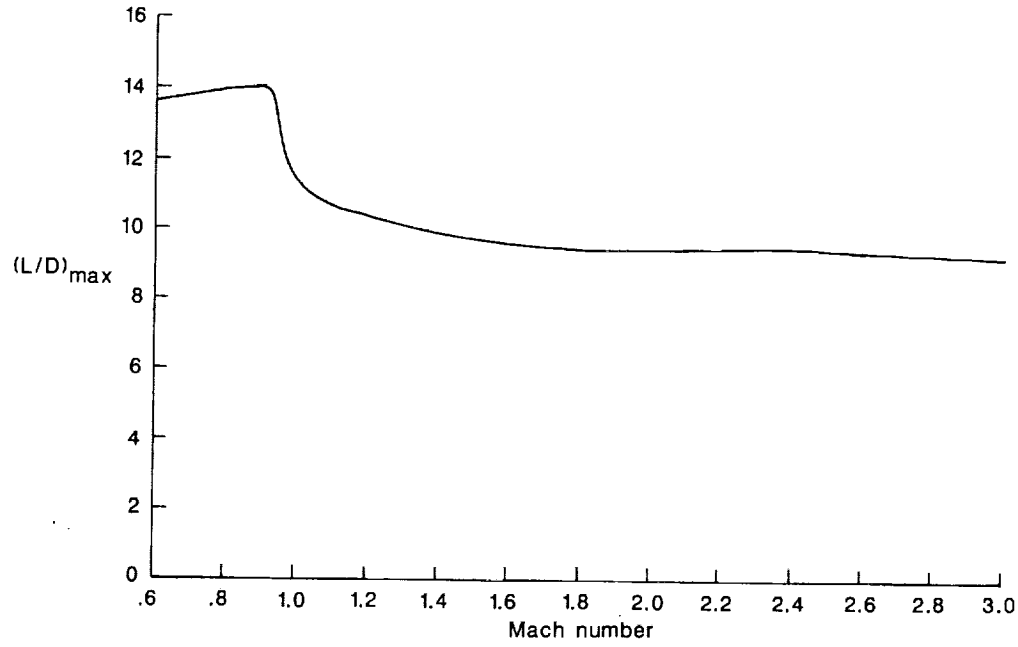

Figure 27. Maximum lift-to-drag ratio as a function of Mach number for baseline aircraft concept.

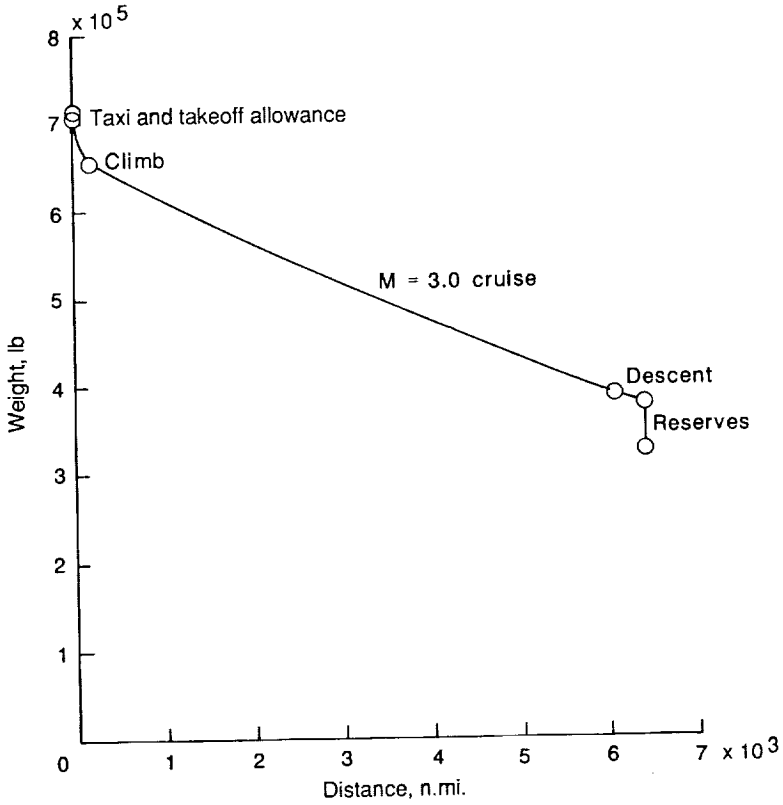

Figure 28. Baseline aircraft instantaneous weight as a function of mission range.

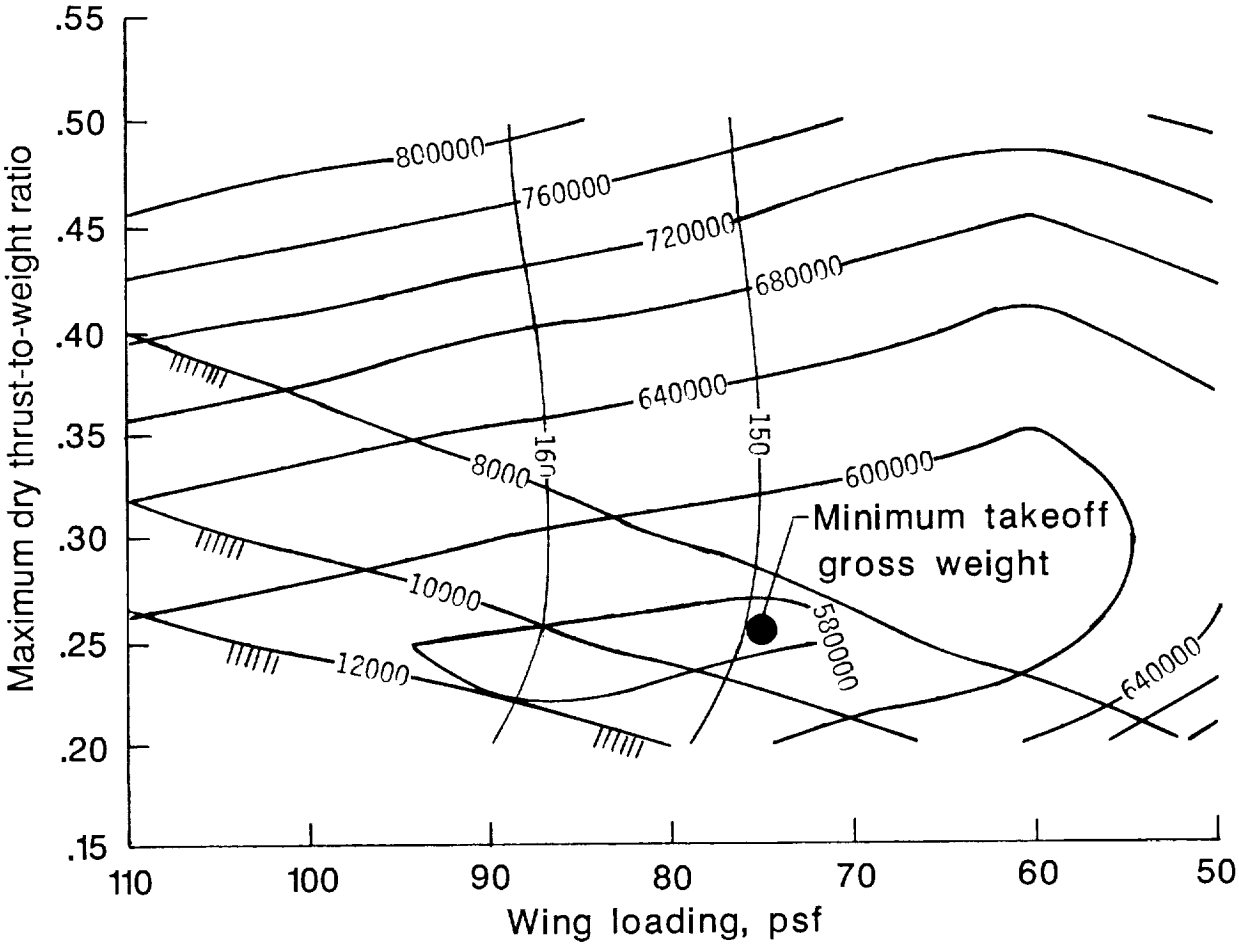

Figure 30. Thumbprint for baseline aircraft configuration using conceptual afterburning turbojet.

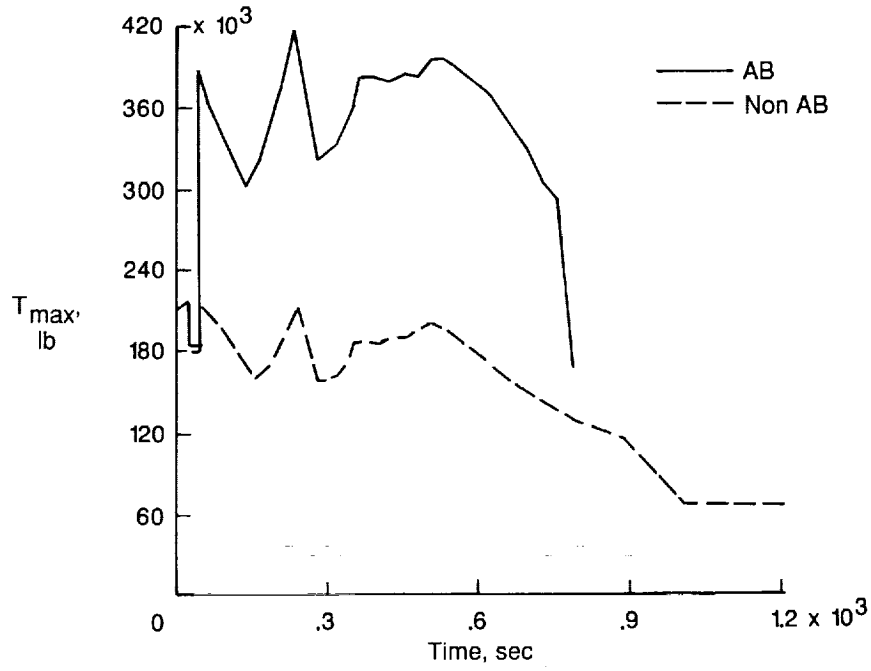

Figure 31. Net climb thrust available for baseline aircraft configuration using conceptual afterburning and nonafterburning turbojets.

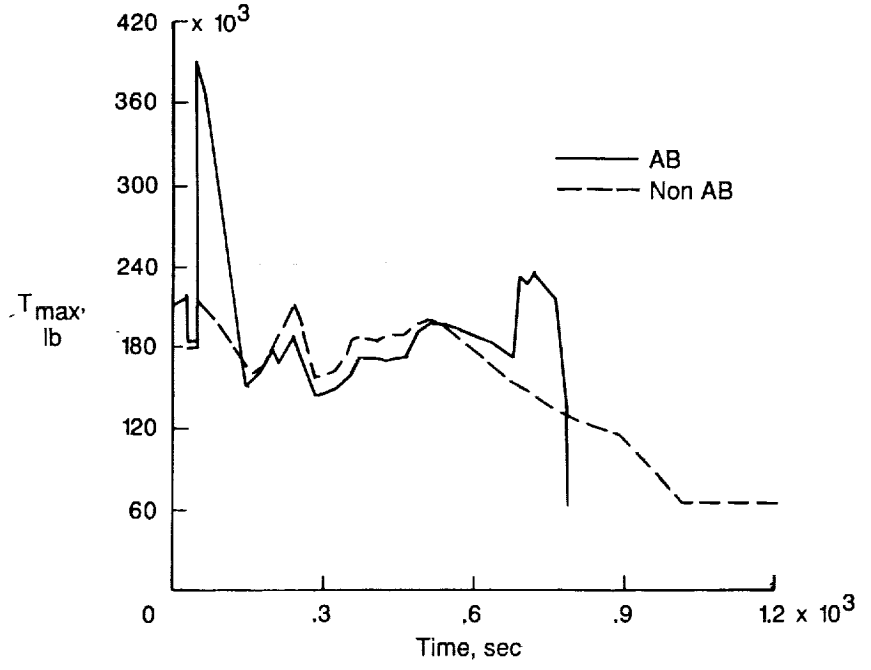

Figure 32. Net climb thrust used (after climb optimization for minimum fuel consumption) for baseline aircraft configuration using conceptual afterburning and nonafterburning turbojets.

NASA
National Aeronautics and Space Administration

Report Documentation Page

1. Report No.	2. Government Accession No.	3. Recipient's Catalog No.
NASA TM-4144		

4. Title and Subtitle
Performance Potential of an Advanced Technology Mach 3 Turbojet Engine Installed on a Conceptual High-Speed Civil Transport

5. Report Date
November 1989

6. Performing Organization Code

7. Author(s)
Shelby J. Morris, Jr., Karl A. Geiselhart, and Peter G. Coen

8. Performing Organization Report No.
L-16531

9. Performing Organization Name and Address
NASA Langley Research Center
Hampton, VA 23665-5225

10. Work Unit No.
505-69-71-03

11. Contract or Grant No.

12. Sponsoring Agency Name and Address
National Aeronautics and Space Administration
Washington, DC 20546-0001

13. Type of Report and Period Covered
Technical Memorandum

14. Sponsoring Agency Code

15. Supplementary Notes
Shelby J. Morris, Jr., and Peter G. Coen: Langley Research Center, Hampton, Virginia.
Karl A. Geiselhart: PRC Kentron, Inc., Aerospace Technologies Division, Hampton, Virginia.

16. Abstract

The performance of an advanced technology conceptual turbojet optimized for a high-speed civil aircraft is presented. This information represents an estimate of performance of a Mach 3 Brayton cycle (gas turbine) engine optimized for minimum fuel burned at supersonic cruise. This conceptual engine had no noise or environmental constraints imposed upon it. The purpose of these data is to define an upper boundary of the propulsion performance for a conceptual commercial Mach 3 transport design. A comparison is presented that demonstrates the impact of the technology proposed for this conceptual engine on the weight and other characteristics of a proposed high-speed civil transport. This comparison indicates that the advanced technology turbojet described in this paper could reduce the gross weight of a hypothetical Mach 3 high-speed civil transport design from about 714 000 lb to about 545 000 lb. The aircraft with the baseline engine and the aircraft with the advanced technology engine are described in this paper.

17. Key Words (Suggested by Authors(s))	18. Distribution Statement
Turbojet Supersonic propulsion Aircraft propulsion and power	Unclassified—Unlimited Subject Category 07

19. Security Classif. (of this report)	20. Security Classif. (of this page)	21. No. of Pages	22. Price
Unclassified	Unclassified	37	A03

NASA FORM 1626 OCT 86

NASA-Langley, 1989

For sale by the National Technical Information Service, Springfield, Virginia 22161-2171